Uncertainties in models of tropospheric ozone based on Monte Carlo analysis: Tropospheric ozone burdens, atmospheric lifetimes and surface distributions

Richard G. Derwent[a]*, David D. Parrish[b,c], Ian E. Galbally[d,e], David S. Stevenson[f], Ruth M. Doherty[f], Vaishali Naik[g], Paul J. Young[h,i]

[a] *rdscientific, Newbury, Berkshire, UK*

[b] *Cooperative Institute for Research in Environmental Sciences, University of Colorado, Boulder, Colorado, USA*

[c] *Chemical Sciences Division, NOAA ESRL, Boulder, Colorado, USA*

[d] *Climate Research Centre, CSIRO Oceans and Atmosphere, Aspendale, Victoria, Australia*

[e] *Australia Centre for Atmospheric Chemistry, School of Chemistry, University of Wollongong, New South Wales, Australia*

[f] *School of GeoSciences, The University of Edinburgh, Edinburgh, UK*

[g] *Geophysical Fluid Dynamics Laboratory, Princeton, New Jersey, USA*

[h] *Lancaster Environment Centre, Lancaster University, Lancaster, UK*

[i] *Data Science Institute, Lancaster University, Lancaster, UK*

* Corresponding author.

E-mail address: r.derwent@btopenworld.com (R.G.Derwent)

1. Introduction

Tropospheric ozone (O_3) is a major policy concern because it is an important pollutant that at elevated levels damages human health and vegetation (Monks et al. 2015). It is also an important radiatively active trace gas that contributes to climate change (IPCC, 2007). As a result, it is the focus of much policy-making activity, the aim of which is to reduce O_3 levels and exposures to meet air quality standards, guidelines or criteria by reducing emissions of its precursors, oxides of nitrogen (NO_x) and volatile organic compounds (VOCs). Sophisticated atmospheric chemistry models are

required to address the complex processes involving O_3 and guide policy-making over the urban to global scales.

While many of the policy-makers' questions on surface ozone can be answered by ozone observations, there are many important policy questions that can only be answered by ozone models. The application of regional-scale air quality models in policy formulation to answer questions concerning reducing ozone levels by reducing precursor emissions, for example, goes back several decades. However, the application of global models to provide policy guidance on tropospheric ozone as a short-lived climate gas and on intercontinental ozone transport is relatively recent (HTAP, 2010). Establishing confidence in global models based on comparison with observations is currently hampered by the dearth of ozone observations.

With the increase in computer power and availability, there has been a tendency to move away from searching for the optimum model and defining the uncertainty in the predictions at that optimum, to performing ensemble experiments. There are different uses of ensembles that could be envisaged within the O_3 subject area, following the discussion and examples described by Beven (2007). The first is the use of ensembles to represent different scenarios of future conditions and this is the approach that has been widely used by the Coupled Model Intercomparison Project (CMIP) (Meehl et al., 2000; IPCC, 2007). The second use of ensembles is to explore the propagation of uncertainties due to input parameters and initial conditions and this approach is widely employed in numerical weather forecasting. The third use of ensembles is to characterise the model response across all model space by running a sample of all possible models and all plausible model input parameters as exemplified in the field of hydrology by Beven and Freer (2001). Ensembles are thus one way of addressing uncertainty, which is a major concern when it comes to O_3 models, the subject of this study.

Here we address those uncertainties within O_3 models that can be dealt with in terms of random variations within model input parameters such as emissions and rate coefficients and their influence

on the O_3 burdens, atmospheric lifetimes and the surface O_3 distribution. This inevitably leaves aside those uncertainties that result from a lack of process-level understanding. We address uncertainties due to model formulation alone by using the results from the Atmospheric Chemistry and Climate Model Intercomparison Project (ACCMIP) (Lamarque et al., 2013; Naik et al., 2013; Stevenson et al., 2013; Young et al., 2013). The aim has been to make a first attempt to quantify the level of uncertainty in O_3 model predictions. Further work will be required to understand whether or not the currently available observational database addressing is adequate enough to assess model performance and to give the required level of confidence in these predictions to policy-makers.

2. Methodology

The methodology adopted in this study aims at preparing a first assessment of the uncertainties in the outputs of current O_3 models. We begin by describing the STOCHEM global Lagrangian chemistry-transport model to which we apply Monte Carlo (MC) uncertainty analysis to the model input parameters that control O_3 precursor emissions and sources and sinks. Then we describe the ACCMIP model ensemble which we use to describe the uncertainties due to model formulation alone. Our focus is on the uncertainties in the tropospheric model estimates of O_3 burdens, lifetimes and surface distributions.

2.1 The STOCHEM model

To address the uncertainties in O_3 models due to model input parameter data, we have employed the global chemistry-transport Stochastic Chemistry (STOCHEM) model. STOCHEM uses a Lagrangian approach in which the atmosphere is divided into a large number (50 000 – 100 000) of air parcels which are advected every three hours by fine resolution winds from the Meteorological Office. A full description of the advection and dispersion processes in STOCHEM is given by Collins et al. (1997). The chemical mechanism in the original STOCHEM model named STOCHEM-OC was replaced with an extended chemistry (Common Representative Intermediates CRI v2-R5) and this version is named STOCHEM-CRI (Utembe et al., 2010; 2011). The original fine resolution meteorological data

employed in the offline STOCHEM-OC and STOCHEM-CRI models were replaced in STOC-HadAM3 (Stevenson et al., 2004) by multiple meteorological fields passed from the Meteorological Office Hadley Centre atmospheric climate model HadAM3 (Pope et al., 2000). The STOC-HadAM3 chemistry – general circulation model contributed to the ACCMIP model study. STOCHEM-OC was employed in the MC uncertainty analyses because of its faster run time. It utilised meteorological fields for 1995 – 1998, close to the year 2000 of the ACCMIP simulations.

Details of STOCHEM-OC are given elsewhere in Derwent et al., (2008) and the references therein. The chemical scheme includes 70 species that take part in 174 thermal chemical and photochemical reactions and utilises a time-step of 5 minutes. Emission fields for a wide range of man-made trace gases including CH_4, CO, NO_x and VOCs were taken for the year 2000. Vegetation emissions of isoprene (C_5H_8) were set at 500 Tg yr^{-1}, lightning NO_x emissions at 5.0 Tg N yr^{-1} and aircraft NO_x emissions at 0.5 Tg N yr^{-1}. The total emissions of methane from wetlands, tundra and rice paddies were set at 260 Tg yr^{-1}. To achieve a situation approaching steady state for ozone, we utilised model experiments covering two years, with one-year spin-up and one full year to capture accurately the seasonal cycles in surface ozone.

Since STOCHEM is a Lagrangian chemistry-transport model, we have access not only to standard gridded output fields of mixing ratios (at coarse resolution 5^o x 5^o x 9 levels) but also to the Lagrangian mixing ratios carried by individual air parcels. In this study, much of the analysis has been performed using these air parcel mixing ratios. At the end of each 3-h advection time-step, the trace gas mixing ratios held by all air parcels within a region defined by a solid angle of 1^o radius around each location of interest were stored. When the model experiments were repeated having changed only the O_3 chemistry, the air parcels took exactly the same paths through the model domain. However, each air parcel carried slightly different mixing ratios in response to the chemistry changes and these could be followed accurately through the MC uncertainty analysis.

2.2 Description of the Monte Carlo analysis of uncertainties

The MC analysis of model input uncertainties has three stages. In the first stage, the uncertainties are described in each STOCHEM-OC model input parameter. In the second stage, the uncertainty range in each model input parameter is sampled quasi-randomly and input values are assigned for all model input parameters for a particular STOCHEM-OC model run. In the third stage, the STOCHEM-OC model is run repeatedly a large number of times, with each run having a different and randomly selected set of input parameters. In this implementation, 98 runs of STOCHEM-OC have been completed, with each model run returning the O_3 burden and atmospheric lifetime, together with the distribution of surface O_3 and its seasonal cycle at three MBL stations.

Table 1 presents the uncertainty ranges assigned to each model input parameter at the initialisation of each model run. Each uncertainty range describes the 1 – 99% (3-σ) confidence range for that parameter. The probability distribution within that range is generally taken to be equally distributed with parameter value on either side of the 'best estimate' (BE), that is to say, it has a 'top hat' shape. For some input parameters, the probability distribution has been assumed to be 'Gaussian' in shape, see Table 1. In all cases, the 3-σ confidence ranges and shapes have been assigned subjectively.

Uncertainties in chemical mechanisms are important sources of uncertainty in global tropospheric ozone models. Chemical kinetic data evaluations (JPL, 2015; IUPAC, 2017) are important sources of information on the uncertainties in reaction rate coefficients and their pressure and temperature dependences, reaction product yields, absorption cross sections and quantum yields. However, they offer limited coverage of the many tens to hundreds of chemical processes represented in global tropospheric ozone models. In this study, chemical mechanism uncertainty is handled by assigning to each thermal rate coefficient and photolysis rate coefficient, an uncertain scaling factor in both the 'inorganic' and 'organic' parts of the mechanism. These scaling factors are taken to be independent of each other and no attempt has been made to address any interactions between the uncertainties in particular rate coefficients that may arise through their laboratory determination or evaluation. We have assumed that each rate coefficient and photolysis rate coefficient has a 3-σ uncertainty

range of ± 35% about their BEs (that is, nominally a factor of two uncertainty range). We based this subjective uncertainty range of close to a factor of two on the recommendation of the IUPAC Subcommittee (Atkinson et al., 2006) for poorly studied reactions. We have also chosen to represent the uncertainty in the rate coefficients only at 298 K and 1 atmosphere pressure and not separately treated uncertainties in temperature and pressure dependences. The IUPAC Subcommittee (Atkinson et al., 2006) recognised that rate coefficients become more uncertain under conditions far removed from 1 atmosphere pressure and 298 K but we were concerned not to make this initial study too complicated. We have chosen not to utilise the uncertainty estimates assigned by the IUPAC Subcommittee because these assignments do not provide comprehensive coverage of the 174 thermal chemical and photochemical rate coefficients in our chemical mechanism. We have also not chosen to treat separately, over and above the factor of two uncertainty range, any dependence of uncertainty in solar zenith angle or stratospheric ozone column.

It is widely accepted that there are important uncertainties associated with global emission inventories of tropospheric ozone precursors from both natural and man-made sources (see for example: Royal Society, 2008 and the references therein). In this initial study, it was not practical to quantify them in detail and so a highly simplistic approach was taken. A scaling factor was applied to each of the global gridded emission fields of NO_x, CO, H_2, CH_4, HCHO, CH_3OH, C_2H_4, C_2H_6, CH_3CHO, C_3H_6, C_3H_8, CH_3COCH_3, C_4H_{10}, C_5H_8, C_7H_8, o-C_8H_{10}, SO_2, CH_3SCH_3, CH_3Br and NH_3 at each point across the globe. These scaling factors were applied at the initialisation of each model run to the BE emission fields taken from Derwent et al. (2008) and were held constant throughout the model run. In this way, uncertainties were assumed to be constant throughout the model domain and independent of time of day and season, although the BE fields themselves were highly spatially and temporally variable. Uncertaintieis were also assumed to be independent of source category, whether man-made, biomass burning, from soils, from oceans or from natural sources. The scaling factors were assigned a 3–σ uncertainty range of ± 30% about their BEs, see Table 1. Our

representation of the emission uncertainties is necessarily rudimentary and merely provides a first rough approximation and guide to further more detailed studies in the future.

At the global scale, O_3 production and loss is controlled by two important meteorological parameters: temperature and water vapour concentrations and by surface deposition. A scaling factor was applied representing bias in the global gridded field of water vapour concentrations. We have assumed that water vapour bias concentrations have a 3–σ uncertainty range of ± 30% about the value calculated from the Met Office meteorological analyses. These scaling factors were assumed to be independent of location, time of day and season. Uncertainties in air temperature were handled by adding a fixed offset or bias term to the temperatures calculated from the Met Office meteorological analyses. This fixed bias had a 3–σ uncertainty range of ± 5 K and 'Gaussian' in shape and was again assumed to be independent of location, time of day and season. Uncertainties in deposition velocities for O_3 and HNO_3 were similarly treated using scaling factors which covered a 3–σ range from 0.65 to 1.35 about the BE.

Having described quantitatively the uncertainty ranges in each of the STOCHEM-OC model input parameters that control the O_3 precursor emissions and the sources and sinks for O_3, then each uncertainty range was sampled quasi-randomly and input parameters were chosen for each STOCHEM-OC model run. STOCHEM-OC was then run with this particular set of model inputs and the output results were stored. In this way, 98 runs of STOCHEM-OC have been completed, each with a different set of inputs, with each model run returning different O_3 burdens, atmospheric lifetimes and surface distributions. Because the only changes made between the 98 runs were to the O_3 sources and sinks, the air parcels took exactly the same paths through the model domain and differences in the model results could be accurately discerned.

2.3 ACCMIP models

ACCMIP consists of a series of time-slice experiments targeting long-term changes in atmospheric composition between 1850 and 2100 (Lamarque et al., 2013). Our focus here has been on the results

of the ACCMIP model simulations of tropospheric ozone and its precursors for the present day, which is taken as the year 2000 time-slice. The fourteen ACCMIP models have a wide range of horizontal and vertical resolutions, vertical extents, chemistry mechanism schemes and parameterisations representing interactions with radiation and clouds. Anthropogenic and biomass burning emissions, though not natural emissions, of O_3 precursors were harmonised as far as possible, bearing in mind the different capabilities of the chemical mechanisms adopted (Lamarque et al., 2013). ACCMIP models and their predictions are described elsewhere (Lamarque et al., 2013; Naik et al, 2013; Stevenson et al., 2013; Young et al., 2013).

In this study, we take the ACCMIP models and their ensemble to provide a reasonable, first attempt to quantify the likely uncertainties in O_3 due to model formulation and structure, including the driving meteorological data or underlying climate model, process descriptions and parameterisations such as chemical mechanisms, whilst all other model inputs were harmonised within reasonable bounds. However, it should be recognised that ACCMIP is an 'ensemble of opportunity' and is not properly constituted to rigorously explore and quantify uncertainty.

2.4 Seasonal cycles in tropospheric ozone at three marine boundary layer stations

Policy-makers can reasonably expect that any model employed in their support is able to faithfully reproduce observations and this is the case for the global O_3 models which are the subject of this study. Observational datasets for O_3 have been authoritatively reviewed by Oltmans et al., (2006) and Cooper et al., (2014). Parrish et al., (2012; 2014) quantified O_3 levels at eleven relatively remote northern midlatitude locations thought to be representative of continental to hemispheric scales. Parrish et al., (2016) compared the seasonal cycles at these locations with the results from three global chemistry-climate models. Derwent et al., (2016) selected three marine boundary layer (MBL) locations out of the eleven and provided a detailed comparison of the observed seasonal cycles with the results from the fourteen ACCMIP models.

Three MBL O_3 monitoring stations were selected for detailed study and comparison with the Monte Carlo and ACCMIP model results here: Mace Head Ireland, Trinidad Head California and Cape Grim Tasmania. Details of these stations and of their baseline records are given in Parrish et al. (2012) and Derwent et al., (2016). To accurately characterise the seasonal cycles in the observations and model predictions, sine curves were fitted through the monthly mean ozone mixing ratios (O_3) using non-linear regression software (NLREG, Sherrod, 1992) which returned five fitted parameters: Y_0, A_1, A_2, ϕ_1 and ϕ_2, representing:

$$O_3 = Y_0 + A_1 \sin(\chi + \phi_1) + A_2 \sin(2\chi + \phi_2) \quad (1)$$

where χ takes the values from 0 to 2π radians in covering one complete year from 1st January to 31st December, Y_0 is the long-term annual average ozone mixing ratio, A_1 and A_2 are the amplitudes of the fundamental and second harmonics and ϕ_1 and ϕ_2 are their phase angles. In all cases the fits and the returned parameters were highly statistically significant. Sets of five parameters were determined for each set of observations for a given marine boundary layer (MBL) monitoring station, for each of the fourteen ACCMIP models using monthly average data and for each of the 98 STOCHEM-OC Monte Carlo runs using the 3-hourly Lagrangian station data.

3. Uncertainties in global burdens and lifetimes for methane, carbon monoxide and ozone

3.1 Monte Carlo replicates

Ninety-eight MC runs were made with STOCHEM-OC and the results for a large number of output variables were collected and ranked in order to provide percentiles, means and standard deviations. The O_3 burden was estimated for each run by summing the O_3 number densities over the model domain and averaging over the last twelve months of each two-year model experiment. As more and more Monte Carlo runs were performed, the spread in the O_3 burdens widened with increasing sample size. So as Figure 1 shows using box-and-whisker plots, the 2 – σ confidence ranges widened from 224 – 502 Tg for the first seven runs, for the first 14, 21 runs and so on, to 192 – 556 Tg for all

98 runs. At the same time, the average O_3 burden changed little from 363 Tg for the first seven runs to 374 Tg for all 98 runs.

The O_3 atmospheric lifetime was estimated for each MC run by dividing the O_3 burden calculated as in the previous paragraph by the total O_3 loss. The total O_3 loss was estimated by summing six separate reaction fluxes over the model domain and over the last twelve months of each two-year model experiment. The six separate fluxes addressed the $OH + O_3$, $HO_2 + O_3$, $O^1D + H_2O$, NO emission, N_2O_5 loss reactions and O_3 dry deposition. The O_3 atmospheric lifetime changed from 22.3 ± 5.1 days (where the quoted range is the 2 – σ or 95% confidence range) for the first seven MC runs to 23.0 ± 8.0 days for all 98 runs.

On this basis, it was concluded that the O_3 burdens and atmospheric lifetimes converged with increasing sample sizes such that convergence was achieved for sample sizes greater than about 20, well below the sample size of 98 actually employed.

These convergence tests were then extended to the tropospheric burdens and atmospheric lifetimes for carbon monoxide (CO) and methane (CH_4). The tropospheric burdens and atmospheric lifetimes for CO only converged for sample sizes greater than about 70, finally settling down to 374 ± 209 Tg and 53 ± 34 days, respectively. The tropospheric burdens and atmospheric lifetimes for CH_4 converged for sample sizes of about 30, midway between O_3 and CO, finally settling down to 4620 ± 460 Tg and 9.0 ± 4.6 years, respectively.

Our results in terms of tropospheric burdens and atmospheric lifetimes for O_3, CO and CH_4 have shown a satisfactory degree of convergence with increasing sample sizes, up to the maximum of 98 for this study. On this basis, these results should provide a first estimate of the likely uncertainty ranges in tropospheric model outputs, driven by uncertainties in O_3 precursor emissions sources and sink processes. There are likely to be diminishing returns in carrying out many more MC runs in order to refine these outputs further. These conclusions are broadly consistent with those found by

Hanna et al., (1998) in their application of MC uncertainty techniques to a large and sophisticated 3-D urban airshed model.

3.2 Comparison between the Monte Carlo runs and the ACCMIP ensemble

STOCHEM-OC model estimates of the global CH_4 burden ranged from 3970 to 5051 Tg, with an average of 4620 ± 460 Tg from the MC analysis. A frequency distribution of the CH_4 burdens indicated a distinct skewness towards larger burdens. This average burden was in reasonable agreement with that from the ACCMIP models (Naik et al., 2013) which gave 4813 ± 162 Tg, see Table 2. Indeed, 40% of the MC runs gave estimates that were within the 2-σ confidence range of the ACCMIP models. However, this agreement is not a crucial test of STOCHEM-OC model performance because of the long CH_4 atmospheric lifetime. The two-year STOCHEM-OC model experiments were not long enough to establish steady state behaviour and so these results were strongly influenced by the chosen initial CH_4 distribution for the year 2000 which was taken from observations (Japan Meterorological Agency, 2012). The apparent agreement with ACCMIP merely confirms that the choice of initial set-up for CH_4 and choice of the one-year spin-up and one-year model experiment represented a reasonable starting point in STOCHEM-OC. Ideally, the Monte Carlo runs should have covered a minimum of ten years to ensure that ozone, carbon monoxide and methane should have reached some form of steady state.

STOCHEM-OC estimates of the CH_4 atmospheric lifetime should be largely free from the influence of the steady state behaviour since it is primarily controlled by the distribution of hydroxyl (OH) radicals in the troposphere. The model estimates ranged from 4.2 to 14.9 years, with an average of 9.0 ± 4.6 years. The frequency distribution showed some evidence of skewness towards longer lifetimes. The average was well within the range of the ACCMIP models which indicated an atmospheric lifetime of 9.7 ± 3.0 years (Naik et al., 2013), see Table 2. Indeed, over 80% of the Monte Carlo model runs gave lifetimes within the 2-σ range of the ACCMIP models. A scatter plot of the CH_4 burden versus the atmospheric lifetime showed good correlation (R^2 = 0.8). The average turnover corresponding to

burden / atmospheric lifetime was 541 ± 228 Tg /year. This estimate corresponded well with the ACCMIP model estimate of 496 ± 154 Tg /year (Naik et al., 2013). The scatter plot showed some evidence of curvature towards long atmospheric lifetimes, indicating underestimation of the CH_4 burdens for those experiments that indicated lifetime in excess of 12 years. This reflects the choices made in fixing the model experimental duration at 2 years.

STOCHEM-OC estimates of the CO burden ranged from 202 Tg to 643 Tg, with an average of 374 ± 209 Tg. These estimates were comparable with those from the ACCMIP models of 323 ± 76 Tg (Naik et al., 2013), see Table 2. Over 70% of the MC model estimates lay within the 2-σ confidence limits of the ACCMIP models. CO atmospheric lifetimes ranged from 24 days to 113 days in the MC runs and showed an average lifetime of 53 ± 34 days. A scatter plot of CO burden against lifetime showed good correlation (R^2 = 0.83) and an average turnover of 7.1 ± 1.7 Tg /day.

STOCHEM-OC estimates for the O_3 burden ranged from 205 Tg to 645 Tg, with an average of 374 ± 182 Tg. A frequency distribution of the model estimates indicated a markedly skewed distribution favouring smaller burdens. These burdens were calculated up to 100 mb and so necessarily included some O_3 that was in the stratosphere. Notwithstanding this, the average burden was in reasonable agreement with that from the ACCMIP models which indicated 337 ± 46 Tg for the troposphere alone (Young et al., 2013), see Table 2. About 40% of the MC runs gave ozone burdens that were within the 2-σ confidence range of the ACCMIP models.

STOCHEM-OC estimates of the O_3 atmospheric lifetime ranged from 15 days to 32 days, with an average of 23 ± 8 days. The frequency distribution of these model values was skewed, with a tail towards longer lifetimes. About 70% of the MC estimates lay within the 2 - σ confidence limits of the ACCMIP models consequently the STOCHEM-OC average was in agreement with that from ACCMIP of 22.3 ± 4 days (Young et al., 2013), see Table 2. A scatter plot of O_3 lifetime versus burden showed reasonable correlation (R^2 = 0.46) and a slope characterised by a turnover of 16.2 ± 6 Tg /day. Again,

this agreed well with the ozone turnover of 15.1 ± 3.4 Tg /day from the subset of the ACCMIP models that provided production and loss diagnostics (Young et al., 2013).

It is concluded from these simple comparisons of the global burdens and atmospheric lifetimes for O_3, CO and CH_4 that the averages of the MC estimates and of the ACCMIP models are in reasonable agreement, taking into account their 2 - σ confidence ranges, see Table 2. Generally, however, the standard deviations are somewhat smaller for the ACCMIP models compared with the MC estimates. This is only to be expected since the ACCMIP models used harmonised emissions data and differed mainly in their meteorological data and model formulations, including chemical mechanisms. In contrast, there has been a conscious effort to describe the uncertainties in the emissions, chemical kinetic and photochemical data employed in the STOCHEM-OC model using MC sampling, albeit with the same model formulation.

4. Seasonal cycles in ozone at MBL stations

The observed and model fitted seasonal cycles in O_3 at Mace Head, Ireland are presented in Figure 2a, showing the results for all 98 MC runs. As reported previously by Parrish et al., (2014), the observed seasonal cycle exhibits a spring-time maximum and a summertime minimum which can be accurately represented using a five parameter sine curve fit as described in section 2.4 above. In contrast, the STOCHEM-OC MC runs exhibited seasonal cycles that exhibited characteristically different behaviour as illustrated in Figure 2a with a tendency to show summertime maxima and wintertime minima. Long-term average Y_0 values converged on 53 ± 21 ppb with increasing sample sizes beyond 50 out of 98, representing a significant overestimate of the observed baseline Y_0 of 38.6 ppb.

Despite comprehensively addressing uncertainties in O_3 precursor emissions and in sources and sinks, few of the MC runs predicted seasonal cycles that satisfactorily matched the Mace Head observations. Whatever the problems were with the STOCHEM-OC model at the Mace Head

location, they could not be fixed by invoking uncertainties in O_3 precursor emissions and sources and sinks.

In contrast, the majority of the ACCMIP models caught accurately the main features of the observed seasonal cycle at Mace Head, Ireland and exhibited well characterised spring-time maxima and summertime minima, see Figure 2b. However, some ACCMIP models gave seasonal cycles that were distinctly different from the observations, showing summertime or wintertime maxima.

Figures 3a and 3b present the observed and model fitted seasonal cycles in O_3 at Trinidad Head, California. Both sets of model averages overestimated the observations but gave broadly similar shaped seasonal cycles. The observed maximum during April was accurately (within one day) predicted by the ACCMIP average but the MC average peaked two weeks later. The observations reached a minimum during July with the MC average reaching a minimum one week earlier and the ACCMIP average two weeks earlier. The observations exhibited a secondary peak during November, the timing of which was well predicted (within 6 days) by the MC average, though the magnitude of the maximum was grossly overestimated. The ACCMIP secondary maximum was also overestimated and was predicted to be one month too early.

The observed and MC model fitted O_3 seasonal cycles at Cape Grim, Tasmania are presented in Figure 4a. The observed seasonal cycle peaked at the end of August, recording 31.7 ppb and reached a minimum during January. The MC runs peaked over a month later and grossly overestimated the observed peak, reaching between 26 – 84 ppb. Each MC curve had a characteristically different shape to that of the observations which meant that the broad features of the observed seasonal cycle were not well predicted by the MC runs. Again, whatever the problems were with the STOCHEM-OC model at the Cape Grim location, they could not be fixed by invoking uncertainties in O_3 precursor emissions and sources and sinks.

The observed and ACCMIP model fitted O_3 seasonal cycles at Cape Grim are presented in Figure 4b. Several of the ACCMIP models showed seasonal cycles that followed the observations closely with

August or September maxima and December or January minima. The ACCMIP average peaked 17 days later compared to the observations but accurately predicted the peak level to within ± 10 %.

Looking in more detail at the values of the five fitted sine curve parameters, then the observed long-term average ozone mixing ratio, Y_0, at Mace Head was well predicted by the ACCMIP models whereas it was less well predicted by the MC runs. The observed Y_0 for Trinidad Head was overestimated by both sets of model predictions. That for Cape Grim was generally well predicted by the ACCMIP models but less well predicted by the MC runs. The observed magnitudes of the amplitudes of the fundamental terms, A_1, were well predicted by both sets of models at Mace Head and Trinidad Head. However, the ACCMIP members tended to underestimate the observed A_1 at Cape Grim and the MC runs tended to overestimate it. The observed fundamental phase angles, ϕ_1, were found to lie within the 2 - σ confidence ranges of the results from the ACCMIP models. However, at all three stations, these predictions spanned an exceedingly wide range of up to nine months. In contrast, the results from the MC replicates were generally tightly distributed but well away from the observed values at all three MBL stations.

The observed amplitudes of the second harmonics, A_2, were generally well predicted by both sets of model predictions. However, the ACCMIP predicted values again spanned a considerable range. The MC runs had difficulty reproducing the observed A_2 at Trinidad Head. The phase angles of the second harmonics, ϕ_2, were again generally well predicted by both sets of model predictions. Again, the ACCMIP predicted values spanned a considerable range and the MC runs had difficulty reproducing the observed ϕ_2 at Trinidad Head. These results are generally consistent with those reported by Derwent et al., (2016), who compared the results of the these same ACCMIP models and the best estimate STOCHEM-CRI model run with the observations from these same three MBL stations.

Despite comprehensively addressing uncertainties in O_3 precursor emissions and in sources and sinks, none of the MC runs gave values of ϕ_1 that matched the observations at any of the three MBL stations. We find it difficult to reconcile the good level of model performance shown by the MC runs

for ϕ_2 at Cape Grim with the poor level shown for A_2 and ϕ_2 at Trinidad Head. However, we could conclude that whatever the problems were with the seasonal cycle at Mace Head, Trinidad Head and Cape Grim in STOCHEM-OC, they could not be fixed by invoking uncertainties in O_3 precursor emissions or production and destruction.

The five fitted parameters obtained from the observations were found to fall within the respective 2-σ confidence ranges calculated for the fourteen ACCMIP members for all three MBL stations. This forms a marked contrast with the situation found for the MC runs. The coverage of model formulation and structure issues, together with meteorological data, across ACCMIP must have been wide enough to ensure that at least one model performed satisfactorily for each of the fitted parameters and at each site. However, it was readily apparent that the ACCMIP member that worked best for one of the five fitted parameters was not necessarily the best for another fitted parameter or for the same parameter at the other site. There was no single ACCMIP member that performed the best for each fitted parameter and site that could in some way be taken as indicating 'best practice' in terms of model formulation and structure.

5. Discussion and Conclusions

We have applied the MC uncertainty approach (see Hanna et al., 1998 and the references therein) to make a first assessment of the uncertainties in one global tropospheric model arising from the uncertainties in O_3 precursor emissions and in the chemical kinetic parameters describing O_3 production and destruction. Estimates of the 2 – σ confidence ranges about the average O_3 burdens and atmospheric lifetimes converged with increasing numbers of MC runs, such that convergence was achieved well within the maximum sample size of 98. The chosen number of MC runs was thus found to be large enough to allow a first estimate to be made of the likely 2 – σ uncertainty ranges in tropospheric parameters. These conclusions applied also to the CO and CH_4 burdens and atmospheric lifetimes. It was further concluded that there would be diminishing returns in carrying

out many more MC runs in order to refine these outputs in terms of averages and 2 – σ confidence ranges.

The MC estimates of O_3 burdens of 374 ± 182 Tg were found to be comparable with those from the ACCMIP models of 337 ± 46 Tg, with the same conclusion found for the atmospheric lifetimes, 23 ± 8 days from the MC runs versus 22.3 ± 4 days from ACCMIP. Generally, the 2 – σ uncertainty ranges were somewhat smaller for the ACCMIP models compared with those for the MC runs. This is only to be expected since the ACCMIP models used harmonised global emission fields and differed only in their meteorological data and model formulations whereas the MC runs covered a wide range in model inputs which addressed uncertainties is both global emissions and chemical kinetic data. On this basis, we conclude that a first estimate has been made of the likely uncertainties in the O_3, CO and CH_4 burdens and atmospheric lifetimes due to uncertainties in global O_3 precursor emissions and in sources and sinks. These uncertainties are between factors of 2 – 4 times larger than those in model formulation alone as revealed by the ranges in the results from ACCMIP.

It is widely accepted that some model input parameters are highly uncertain (Young et al., 2018), to the extent that the assumptions made here of a factor of two uncertainty range may underestimate the actual uncertainty. If global models were particularly sensitive to such parameters then this study would necessarily have underestimated the uncertainty ranges in the model output variables studied. In such a case then, the uncertainty range due to uncertain input parameters would be greater than that from the spread of different models. In general, when discussed, “model uncertainty” is determined from the spread of results from different models – i.e. uncertainty due to model formulation (e.g. Hawkins and Sutton, 2009; Young et al., 2013). Support for this has previously come from comparing the ensemble spread of CMIP5 (Coupled Model Intercomparison Project – Phase 5) climate models against perturbed physics and initial condition ensembles from single models, with the single model ensembles showing less dispersion than the multi-model ones (Yokohata et al., 2013). However, here there is a wider uncertainty range found for the STOCHEM-

OC (single model) ensemble compared with ACCMIP multi-model ensemble. This is likely due to the comparatively large parameter ranges explored in the STOCHEM-OC MC runs but this point should be revisited with other global chemistry models to see if their uncertainty range is also greater than a multi-model spread.

The seasonal cycles in surface O_3 were assembled from both the MC runs and the fourteen ACCMIP models for the 2000s time-slice and compared with the seasonal cycles at the three MBL stations. Detailed examination of the predicted and observed seasonal cycles was achieved by fitting sine curves through the seasonal cycles and determining five fitted parameters: the long-term average, Y_0, and A_1 and ϕ_1, to define the fundamental and A_2 and ϕ_2 to define the second harmonic. These five parameters were determined for the available observations, all 98 MC runs and all fourteen ACCMIP members for the three MBL stations. A close examination of these fitted parameters showed that the broad level of agreement found in a cursory examination of the model output was illusory. That is to say, although the long-term average Y_0 values were in reasonable agreement with the observed values, this was not always the case for the A_1, ϕ_1, A_2 and ϕ_2 values at each of the MBL stations.

We found it difficult to reconcile the good level of model performance shown by the MC runs for some fitted parameters at some stations with the poor level shown by at other stations. Because the uncertainties applied to the BE runs were largely independent of time of day and season, it is possible that the MC runs would not produce strong changes in seasonal cycles at the MBL stations. However, although the perturbations were largely constant in time and space, they operated on BE processes describing ozone production and destruction that were highly variable both spatially and temporally. We therefore concluded that whatever the problems were with the representation of the seasonal cycle in ozone at the three MBL stations in STOCHEM-OC, they could not be fixed by invoking uncertainties in O_3 precursor emissions and in the chemical kinetic parameters defining O_3 production and destruction.

The observed values of each of the five fitted parameters were found to fall within the respective 2-σ confidence ranges calculated for the 14 ACCMIP members. The coverage of model formulation and structure issues, together with meteorological data, across ACCMIP must have been wide enough to ensure that at least one model performed satisfactorily for each of the fitted parameters and at each site. All the features of the O_3 seasonal cycles at the three MBL stations were achievable across the range of the ACCMIP members but they were not achievable within a single model. Consequently, we are unable to explain which features of the ACCMIP members led to good performance and which led to poor performance.

A number of explanations have been considered for the poor performance of STOCHEM-OC in predicting ozone at MBL stations. There is the possibility that the chosen value for the deposition velocity of O_3 to ocean surfaces may have been underestimated leading to an underestimation of deposition to the southern oceans which would particularly affect the predictions for Cape Grim, situated as it is on the western coast of Tasmania. Increasing the deposition velocity decreased the over-estimation in O_3 but made no change to the shape of the seasonal cycles. Such an increase in the deposition velocity of O_3 to the oceans would be contrary to current developments in the oceanic dry deposition of O_3 (Luhar et al., 2017). There is a further possibility that a photochemically-labile halogen species is emitted from the ocean surface and may destroy O_3 photochemically (Dickerson et al., 1999). Making some plausible assumptions concerning possible ocean sources controlled by sea-surface temperatures again merely decreased the model overestimation without inducing noticeable changes in the shapes of the seasonal cycles. No further model experiments were performed to pursue these possibilities.

A major uncertainty in the modelling of tropospheric composition lies in the transport of chemical species and its representation in current models (Orbe et al., 2016). Orbe et al., (2016) identify two approaches to reducing uncertainty in atmospheric transport either by using winds from meteorological analyses directly in a chemistry-transport model or by constraining the flow in a

general circulation model. Both approaches were apparent in ACCMIP (Lamarque et al., 2013). In addition to the uncertainties associated with the use of analysed winds, there are additional uncertainties arising from the parameterisations used to represent deep convection, gravity wave drag and the atmospheric boundary layer (Lawrence et al., 2003; Doherty et al., 2005; Rind et al., 2007; Orbe et al., 2016). Whilst a detailed examination of all of these issues is beyond the scope of this study, we note the importance of the uncertainties arising from the parameterisation of deep convection and why they may be of particular concern in the context of the present study of the O_3 seasonal cycles at MBL stations.

In previous studies, Parrish et al., (2016) have noted the importance of the issue of the isolation of the marine boundary layer from the free troposphere in establishing the observed seasonal cycle in ozone at the surface. So, in particular above the Trinidad Head site in the altitude range from the surface to 3 km, the peak of the fundamental term of the seasonal cycle shifts from March to June, that is to say, ϕ_1, decreases from about 0.5 to < -1 radians. In the STOCHEM-OC model, convective mixing wiped out the isolation of the marine boundary layer bringing the seasonal cycle of the free troposphere down to the surface model layer and giving a similar seasonal cycle over the 950 – 550 mb layer. At the Cape Grim site, observed O_3 peaks during August to September whilst O_3 at an altitude of 2 km peaks during December – January implying a marked change in the ozone seasonal cycle in the lower troposphere. Again, this change is not reproduced by STOCHEM-OC, which accurately reproduced the seasonal cycle in the free troposphere but wrongly carried this all the way down the altitude profile to the surface.

It is therefore possible that the different choices made of the parameterisations for deep convection within the ACCMIP models account for their inconsistent performance when evaluated against the observed O_3 seasonal cycles. Furthermore, the parameterisation of convective mixing in STOCHEM-OC may have led to an overestimation of mixing which has eroded the isolation of the marine boundary layer above both sites and thus hid the model's real level of performance for free

tropospheric O_3. Further sensitivity experiments are thus called for across the range of tropospheric models employed for policy purposes to examine the importance of the parameterisation of convective mixing and its influence on the O_3 seasonal cycle at MBL stations.

Acknowledgements

The authors are grateful to P.G. Simmonds and T.G. Spain for providing the Mace Head data and for A.J. Manning for sorting the Mace Head data into baseline and non-baseline observations. The data analysed here are available from the authors. ACCMIP was organised under the auspices of the International Global Atmospheric Chemistry (IGAC) and Stratosphere-Troposphere Processes And their Role in Climate (SPARC) projects. The authors are grateful to the British Atmospheric Data Centre (BADC), which is part of the NERC National Centre for Atmospheric Science (NCAS), for collecting and archiving the ACCMIP data.

D. Parrish acknowledges support from NOAA's Climate Program Office.

R. Derwent acknowledges support from the Department for Energy and Climate Change UK, under contract CESA 002 and from Department for Environment, Food and Rural Affairs UK for the development of STOCHEM and the CRI mechanism.

References

Atkinson, R., Cox, R.A., Crowley, J.N., Hampson, R.F., Hynes, R.G., Jenkin, M.E., Kerr, J.A., Rossi, M.J., Troe, J., 2006. Summary of evaluated kinetic and photochemical data for atmospheric chemistry. Web version October 2006, Centre for Atmospheric Science, Cambridge, UK.

Beven, K., 2009. Environmental modelling: An uncertain future. Routledge, Oxfordshire.

Beven, K., Freer, J., 2001. Equifinality, data assimilation, and uncertainty estimation in mechanistic modelling of complex environmental systems using the GLUE methodology. Journal of Hydrology 249, 11-29.

Collins, W.J., Stevenson, D.S., Johnson, C.E., Derwent R.G., 1997. Tropospheric ozone in a global-scale three-dimensional Lagrangian model and its response to NO_x emission controls. Journal of Atmospheric Chemistry 26, 223-274.

Cooper, O.R., Parrish, D.D., Ziemke, J., Balashov, N.V., Cupeiro, M., Galbally, I.E., Gilge, S., Horowitz, L., Jensen, N.R., Lamarque, J.-F., Naik, V., Oltmans, S.J., Schwab, J., Shindell, D.T., Thompson, A.M., Thouret, V., Wang, Y., Zbinden, R.M., 2014. Global distribution and trends of tropospheric ozone: An observation-based review. Elementa: Science of the Anthropocene 2, 1-28, doi:10.12952/journal.elementa.000029.elementascience.org.

Derwent, R.G., Stevenson, D.S., Doherty, R.M., Collins, W.J., Sanderson, M.G., 2008. How is surface ozone in Europe linked to Asiana and North American NO_x emissions? Atmospheric Environment 7412-7422.

Derwent, R.G., Parrish, D.D., Galbally, I.E., Stevenson, D.S., Doherty, R.M., Young, P.J., Shallcross, D.E., 2016. Interhemispheric differences in seasonal cycles of tropospheric ozone in the marine boundary layer: Observation-model comparisons. Journal of Geophysical Research: Atmospheres 121, doi:10.1002/2016JD024836.

Dickerson, R.R., Rhoads, K.P., Carsey, T.P., Oltmans, S.J., Burrows, J.P., Crutzen, P.J., 1999. Ozone in the remote marine boundary layer: A possible role for halogens. Journal of Geophysical Research 104, D107, 21385-21395.

Doherty, R.M., Stevenson, D.S., Collins, W.J., and Sanderson, M.G., 2005. Influence of convective transport on tropospheric ozone and its precursors in a chemistry-climate model. Atmospheric Chemistry and Physics 5, 3205-3218.

Hanna, S.R., Chang, J.C., Fernau, M.E., 1998. Monte Carlo estimates of uncertainties in predictions by a photochemical grid model (UAM-IV) due to uncertainties in input variable. Atmospheric Environment 32, 3619-3628.

Hawkins, E., Sutton, R., 2009. The potential to narrow uncertainty in regional climate model predictions. Bulletin of the American Meteorological Society 90, 1095-1107.

HTAP, 2010. Hemispheric transport of air pollution 2010. Part A.: ozone and particulate matter. Air Pollution Studies No. 17. United Nations, Geneva, Switzerland.

IPCC, 2007. Summary for policymakers, in: Climate Change 2007: The Physical Science Basis. Cambridge University Press, Cambridge, UK.

IUPAC, 2017. Task Group on atmospheric chemical kinetic data evaluation. http://iupac.pole-ether.fr.

Japan Meteorological Agency, 2012. WMO WDCGG Data Summary. WDCGG No. 36, Japan Meteorological Agency, Japan.

JPL, 2015. Chemical kinetics and photochemical data for use in atmospheric studies. Evaluation number 18. Jet Propulsion Laboratory, Pasadena, USA. https://jpldataeval.jpl.nasa.gov/pdf/JPL_Publication_15-10.pdf.

Lamarque, J.-F., Shindell, D.T., Josse, B., Young, P.J., Cionni, I., Eyring, V., Bergmann, D., Cameron-Smith, P., Collins, W.J., Doherty, R., Dalsoren, S., Faluvegi, G., Folberth, G., Ghan, S.J., Horowitz, L.W., Lee, Y.H., MacKenzie, I.A., Nagashima, T., Naik, V., Plummer, D., Righi, M., Rumbold, S.T., Schulz, M., Skeie, R.B., Stevenson, D.S., Strode, S., Sudo, K., Szopa, S., Voulgarakis, A., Zeng, G., 2013. The Atmospheric Chemistry and Climate Model Intercomparison Project (ACCMIP): overview and description of models, simulations and climate diagnostics. Geoscience Model Development 6, 179-206.

Lawrence, M.G.R., von Kuhlmann, M., Salzmann, M., Rasch, P.J., 2003. The balance of effects of deep convective mixing on tropospheric ozone. Geophysical Research Letters 30, 1940, doi:10.1029/2003GL017644.

Luhar, A.K., Galbally, I.E., Woodhouse, M.T., Thatcher, M., 2017. An improved parameterization of ozone dry deposition to the ocean and its impact in a global climate-chemistry model. Atmospheric Chemistry and Physics 17, 3749-3767.

Meehl, G.A., Boer, G.J., Covey, C., Latif, M., Stoufer, R.J., 2000. The Coupled Model Intercomparison Project (CMIP). Bulletin of the American Meteorological Society 81, 313-318.

Monks, P.S., Archibald, A.T., Colette, A., Cooper, O., Coyle, M., Derwent, R., Fowler, D., Granier, C., Law, K.S., Mills, G.E., Stevenson, D.S., Tarasova, O., Thouret, V., von Schneidemesser, E., Sommariva, R., Wild, O., Williams, M.L., 2015. Tropospheric ozone and its precursors from the urban to the global scale from air quality to short-lived climate forcer. Atmospheric Chemistry and Physics 15, 8889-8973.

Naik, V., Voulgarakis, A., Fiore, A.M., Horowitz, L.W., Lamarque, J.-F., lin, M., Prather, M.J., Young, P.J., Bergmann, D., Cameron-Smith, Cionni, I., Collins, W.J., Dalsoren, S.B., Doherty, R., Eyring, V., Faluvegi, G., Folberth, G.A., Josse, B., Lee, Y.H., MacKenzie, I.A., Nagashima, T., van Noije, T.P.C., Plummer, D.A., Righi, M., Rumbold, S.T., Skeie, R., Shindell, D.T., Stevenson, D.S., Strode, S., Sudo, K., Szopa, S., Zeng, G., 2013. Pre-industrial to present-day changes in tropospheric hydroxyl and methane lifetime from the Atmospheric Chemistry and Climate Model Intercomparison Project (ACCMIP). Atmospheric Chemistry and Physics 13, 5277-5298.

Oltmans, S., Lefohn, A.S., Harris, J.M., Galbally, I.E., Scheel, H.E., Bodekerf, G., Brunke, E., Claude, H., Tarasick, D., Johnson, B.J., Simmonds, P.G., Shadwick, D., Anlauf, K., Hayden, K., Schmidlin, F., Fujimoto, T., Akagi, K., Meyer, C., Nichol, S., Davies, J., Redonda, A., Cuevas, E., 2006. Long-term changes in tropospheric ozone. Atmospheric Environment 40, 3156-3173.

Orbe, C., Waugh, D.W., Yang, H., Lamarque, J.-F., Times, S., Kinnison, D.E., 2016. Tropospheric transport differences between models using the same large-scale meteorological fields. Geophysical Research Letters 44, 1068-1078, doi:10.1002/2016GL071339.

Parrish, D.D., Law, K.S., Staehelin, J., Derwent, R., Cooper, O.R., Tanimoto, H., Volz-Thomas, A., Gilge, S., Scheel, H.-E., Steinbacher, M., Chan, E., 2012. Long-term changes in lower tropospheric baseline

ozone concentrations at northern mid-latitudes. Atmospheric Chemistry and Physics 12, 11,485-11,504.

Parrish, D.D., Lamarque, J.-F., Naik, V., Horowitz, L., Shindell, D.T., Staehelin, J. Derwent, R., Cooper, O.R., Tanimoto, H., Volz-Thomas, A., Gilge, S., Scheel, H.-E., Steinbacher, M., Frohlich, M., 2014. Long-term changes in lower tropospheric baseline ozone concentrations: Comparing chemistry-climate models and observations at northern latitudes. Journal of Geophysical Research 119, 5719-5736, doi:10.1002/2013JD021435.

Parrish, D.D., Galbally, I.E., Lamarque, J.-F., Naik, V., Horowitz, L., Shindell, D.T., Oltmans, S.J., Derwent, R.G., Tanimoto, H., Labuschagne, C., Cupeiro, M., 2016. Seasonal cycles of O_3 in the marine boundary layer: Observation and model simulation comparisons. Journal of Geophysical Research: Atmospheres 121, 538-557, doi:10.1002/2015JD024101.

Pope, V.D., Gallani, M.L., Rowntree, P.R., Stratton, R.A., 2000. The impact of new physical parameterizations in the Hadley Centre climate model: HadAM3. Climate Dynamics 16, 123-146.

Rind, D., lerner, J., Jonas, J., McLinden, C., 2007. Effects of resolution and model physics on tracer transports in the NASA Goddard Institue for Space Studies general circulation models. Journal of Geophysical Research 112, D09315, doi:10.1029/2006JD007476.

Royal Society, 2008. Ground-level ozone in the 21st century: Future trends, impacts and policy implications. Science Policy Report 15/08, Royal Society, London.

Sherrod, 1992. NLREG software. http://www.nlreg.com.

Stevenson, D.S., Doherty, R.M., Sanderson, M.G., Collins, W.J., Johnson, C.E., Derwent. R.G., 2004. Radiative forcing from aircraft NOx emissions: mechanisms and seasonal dependence. Journal of Geophysical Research 109, D17307, doi:10.1029/2004JD004759.

Stevenson, D.S., Young, P. J., Naik, V., Lamarque, J.-F., Shindell, D.T., Voulgarakis, A., Skeie, R. B., Dalsoren, S. B., Myhre, G., Berntsen, T. K., Folberth, G. A., Rumbold, S. T., Collins, W. J., MacKenzie, I.

A., Doherty, R. M., Zeng, G., van Noije, T. P. C., Strunk, A., Bergmann, D., Cameron-Smith, D., Plummer, D.A., Strode, S. A., Horowitz, L., Lee, Y. H., S., Sudo, K., Nagashima, T., Josse, B., Cionni, I., Righi, M., Eyring, V., Conley, A., Bowman, K. W., Wild, O., Archibald, A., 2013. Tropospheric ozone changes, radiative forcing and attribution to emissions in the Atmospheric Chemistry and Climate Model Intercomparison Project (ACCMIP). Atmospheric Chemistry and Physics 13, 3063-3085.

Utembe, S.R., Cooke, M.C., Archibald, A.T., Jenkin, M.E., Derwent, R.G., Shallcross D.E., 2010. Using a reduced Common Representative Intermediates (CRI v2-R5) mechanism to simulate tropospheric ozone in a 3-D Lagrangian chemistry transport model. Atmospheric Enviroment. 13, 1609-1622.

Utembe, S.R., Cooke, M.C., Archibald, A.T., Shallcross, D.E., Derwent, R.G., Jenkin, M.E., 2011. Simulating secondary organic aerosol in a 3-D Lagrangian chemistry transport model using the reduced Common Representative Intermediate mechanism (CRI v2-R5). Atmospheric Environment 45, 1604-1614.

Yokohata, T., Annan, J.D., Collins, M., Jackson, C.S., Shiogama, H., Watanabe, M., Emori, S., Yoshimori, M., Abe, M., Webb, M.J., Hargreaves, J.C., 2013. Reliability and importance of structural diversity of climate model ensembles. Climate Dynamics 41, 2745-2763.

Young, P.J., Archibald, A.T., Bowman, K.W., Lamarque, J.-F., Naik, V., Stevenson, D.S., Tilmes, S., Voulgarakis, A., Wild, O., Bergmann, D., Cameron-Smith, P., Cionni, I., Collins, W.J., Dalsoren, S.B., Doherty, R.M., Eyring, V., Faluvegi, G., Horowitz, L.W., Josse, B., Lee, Y.H., MacKenzie, I.A., Nagashima, T., Plummer, D.A., Righi, M., Rumbold, S.T., Skeie, R.B., Shindell, D.T., Strode, S.A., Sudo, K., Szopa, S., Zeng, G., 2013. Pre-industrial to end 21st century projections of tropospheric ozone from the Atmospheric Chemistry and Climate Model Intercomparison Project (ACCMIP). Atmospheric Chemistry and Physics 13, 2063-2090.

Young, P.J., Naik, V., Fiore, A.M., Gaudel, A., Guo. J., Lin, M.Y., et al., 2018. Tropospheric Ozone Assessment Report: Assessment of global-scale model performance for global and regional ozone

distributions, variability and trends. Elementa: Science of the Anthropocene 6, Article 10, doi:10.1525/elementa.265.

Table 1. Representation of the uncertainties in the STOCHEM-OC model input parameters in the Monte Carlo study of input parameter uncertainties.

Input parameter	Representation	Range
31 inorganic rate coefficients	multiplicative scaling	x 0.65 – 1.35
11 RO_2+NO rate coefficients	multiplicative scaling	x 0.65 – 1.35
16 RO_2+RO_2 rate coefficients	multiplicative scaling	x 0.65 – 1.35
8 RO_2+HO_2 rate coefficients	multiplicative scaling	x 0.65 – 1.35
25 OH+VOC rate coefficients	multiplicative scaling	x 0.65 – 1.35
8 photolysis rate coefficients	multiplicative scaling	x 0.65 – 1.35
Temperature	additive	± 0 – 5 K
Water vapour	multiplicative scaling	x 0.65 – 1.35
O_3 dry deposition velocity	multiplicative scaling	x 0.65 – 1.35
HNO_3 dry deposition velocity	multiplicative scaling	x 0.65 – 1.35
NO_x emissions	multiplicative scaling	x 0.65 – 1.35
CO emissions	multiplicative scaling	x 0.65 – 1.35
H_2 emissions	multiplicative scaling	x 0.65 – 1.35
SO_2 emissions	multiplicative scaling	x 0.65 – 1.35
DMS emissions	multiplicative scaling	x 0.65 – 1.35
ammonia emissions	multiplicative scaling	x 0.65 – 1.35
CH_3Br emissions	multiplicative scaling	x 0.65 – 1.35
methane emissions	multiplicative scaling	x 0.65 – 1.35
methanol emissions	multiplicative scaling	x 0.65 – 1.35
HCHO emissions	multiplicative scaling	x 0.65 – 1.35
ethane emissions	multiplicative scaling	x 0.65 – 1.35
ethylene emissions	multiplicative scaling	x 0.65 – 1.35
CH_3CHO emissions	multiplicative scaling	x 0.65 – 1.35
propane emissions	multiplicative scaling	x 0.65 – 1.35
propylene emissions	multiplicative scaling	x 0.65 – 1.35
acetone emissions	multiplicative scaling	x 0.65 – 1.35
butane emissions	multiplicative scaling	x 0.65 – 1.35
isoprene emissions	multiplicative scaling	x 0.65 – 1.35
toluene emissions	multiplicative scaling	x 0.65 – 1.35
o-xylene emissions	multiplicative scaling	x 0.65 – 1.35

Notes:

a. all assignments in this table are subjective;

b. a scaling factor of unity represents ‘best estimate’.

Table 2. Comparison of the burdens and lifetimes for ozone, carbon monoxide and methane from the Monte Carlo runs and from ACCMIP.

Trace gas	Monte Carlo runs	ACCMIP
ozone burden in Tg	374 ± 182	337 ± 46[a]
ozone lifetime in days	23.0 ± 8	22.3 ± 4[a]
carbon monoxide burden in Tg	374 ± 209	323 ± 76[b]
carbon monoxide lifetime in days	53 ± 34	
methane burden in Tg	4620 ± 460	4813 ± 162[b]
methane lifetime in years	9.0 ± 4.6	9.7 ± 3.0[a]

Notes:

[a.] Young et al., 2013

[b.] Naik et al., 2013.

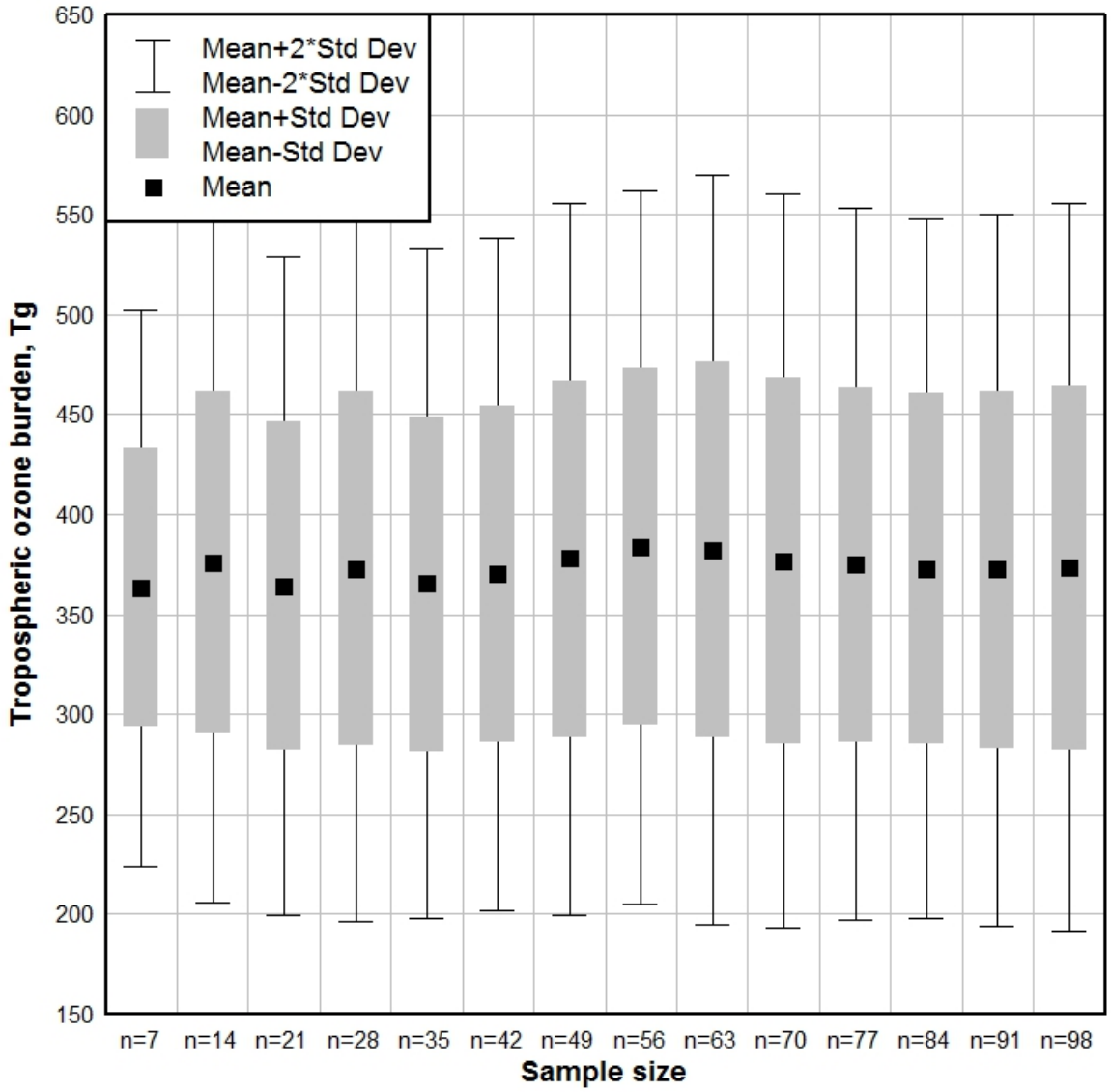

Figure 1. Box-and-whisker plot of the uncertainty distribution of the O_3 burdens found in the STOCHEM-OC Monte Carlo model runs with increasing sample size. The black squares show the average values, the grey rectangles show the 1 – σ confidence ranges and the whiskers the 2 – σ confidence ranges.

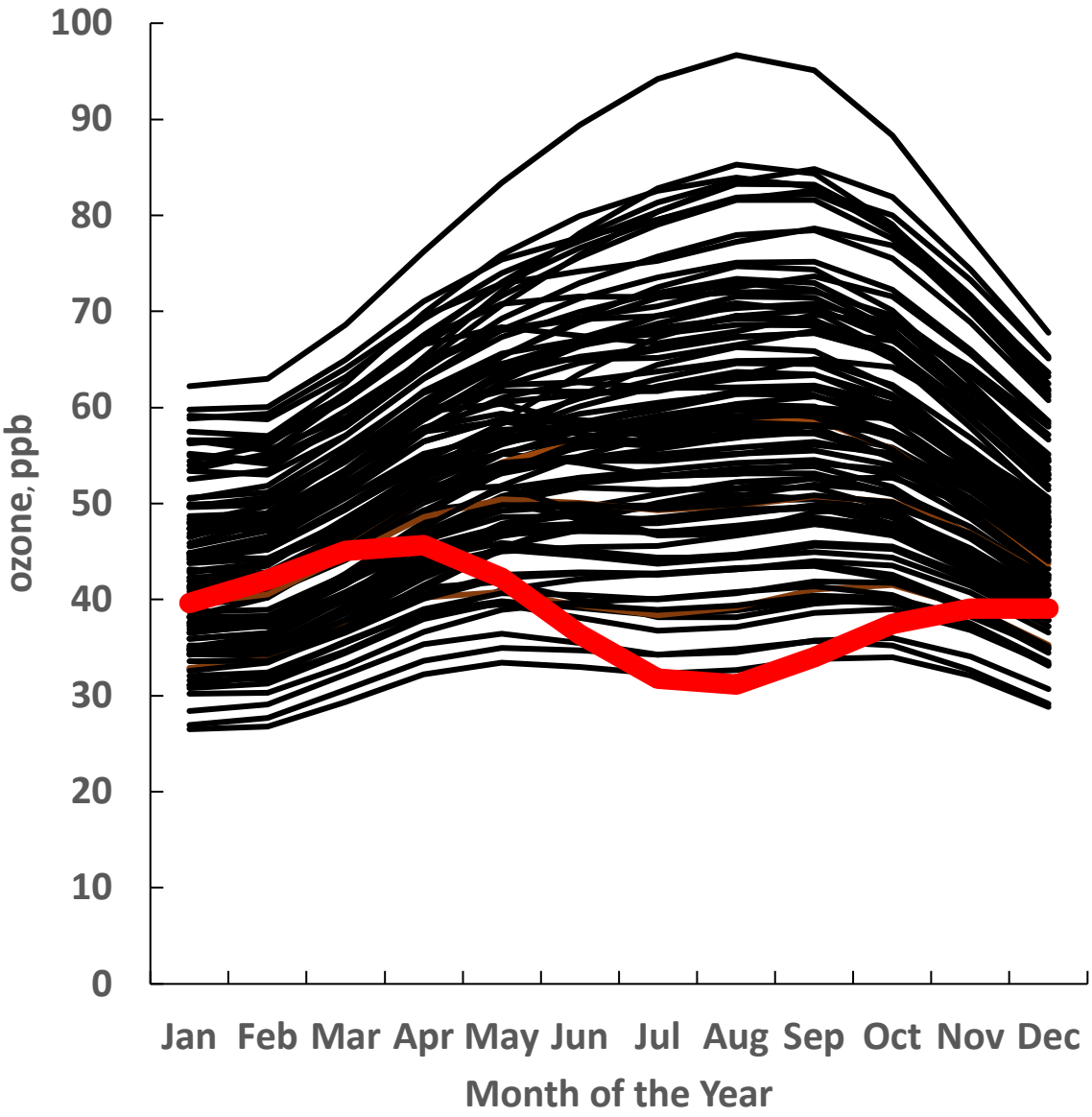

Figure 2a. Seasonal cycles in ozone at the Mace Head, Ireland marine boundary layer station in the STOCHEM-OC Monte Carlo model runs (black lines) and in the observations (thick red line).

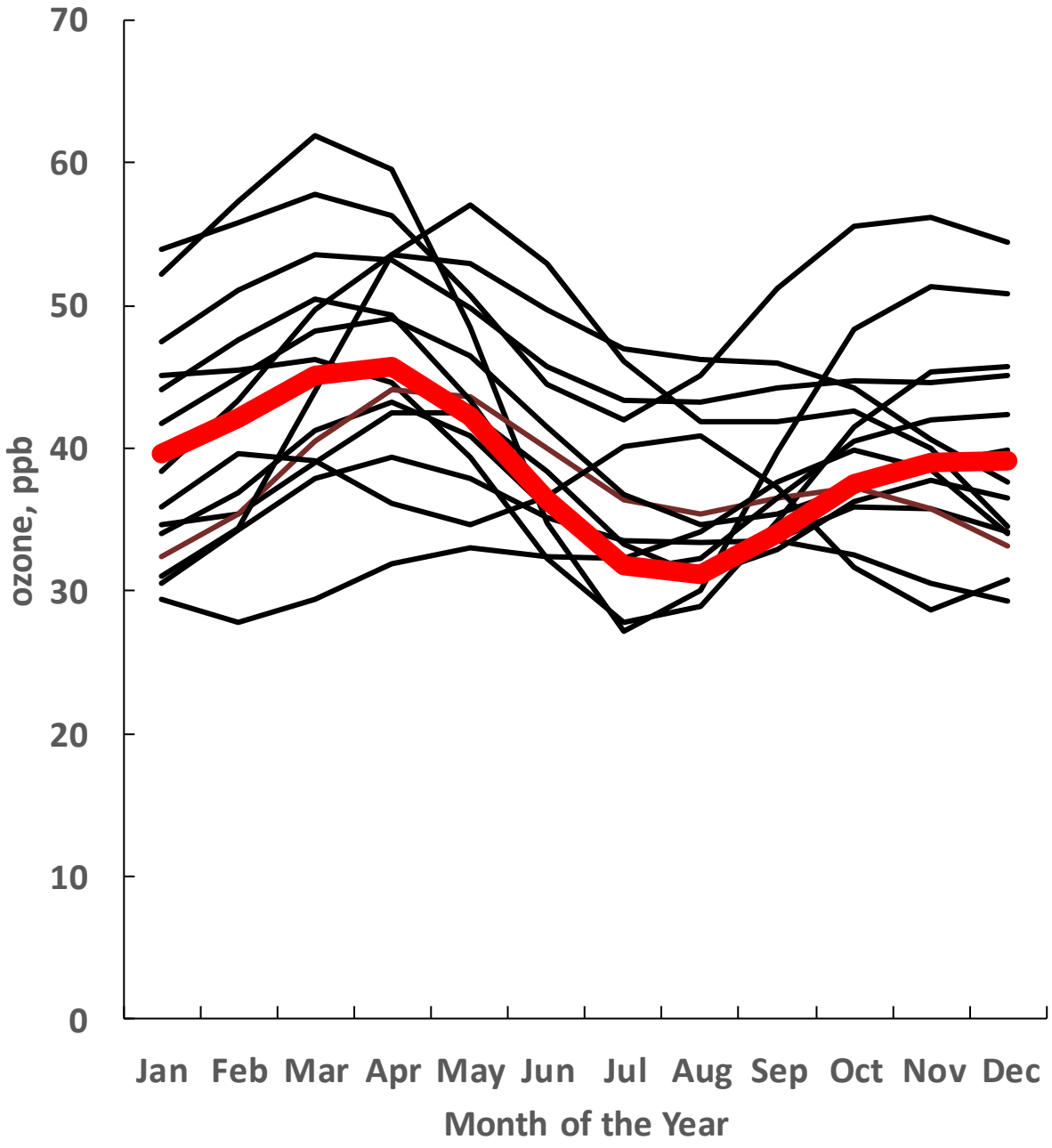

Figure 2b. Seasonal cycles in ozone at the Mace Head, Ireland marine boundary layer station in the ACCMIP models (black lines) and in the observations (thick red line).

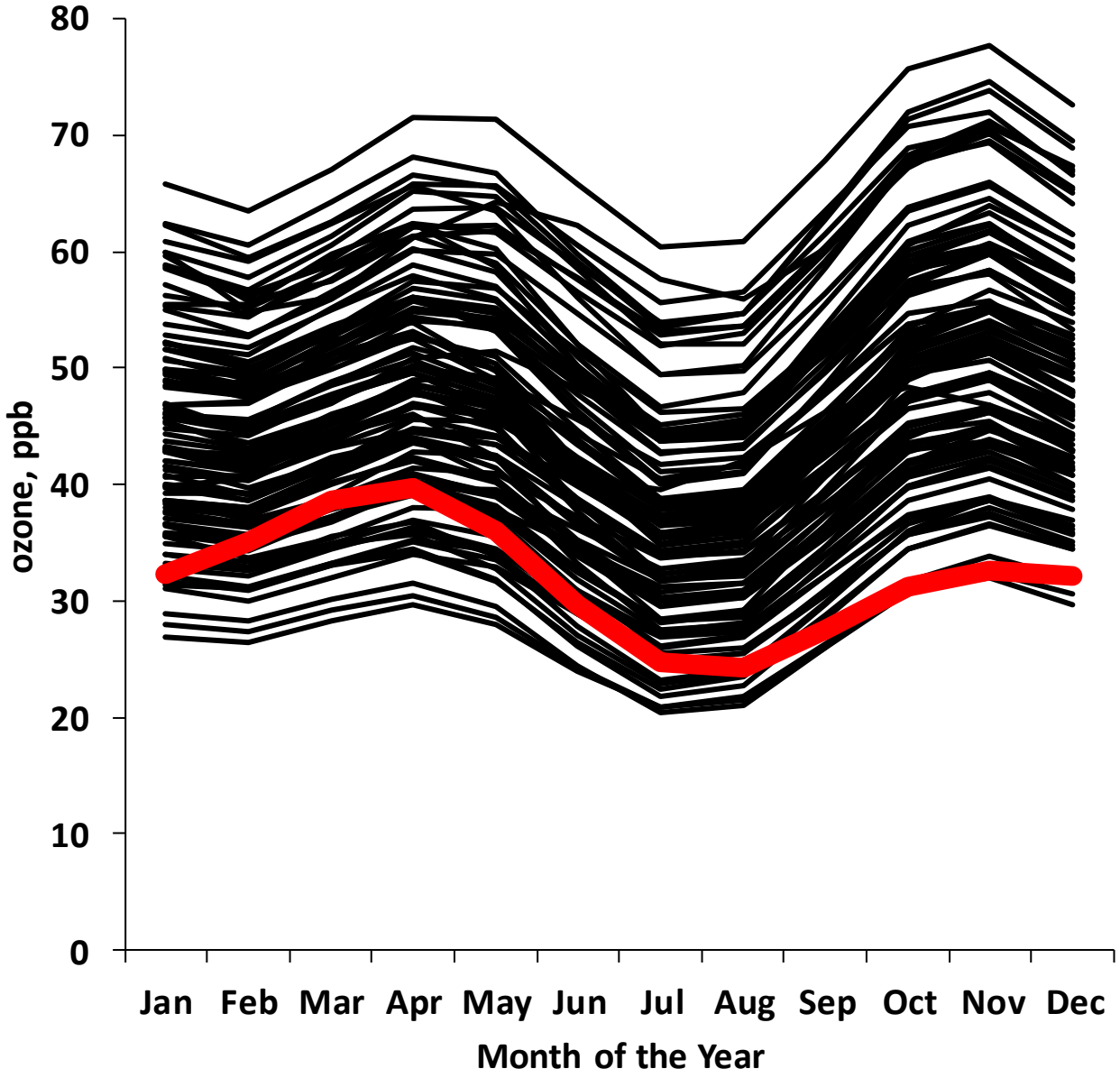

Figure 3a. Seasonal cycles in ozone at the Trinidad Head, California marine boundary layer station in the STOCHEM-OC Monte Carlo model runs (black lines) and in the observations (thick red line).

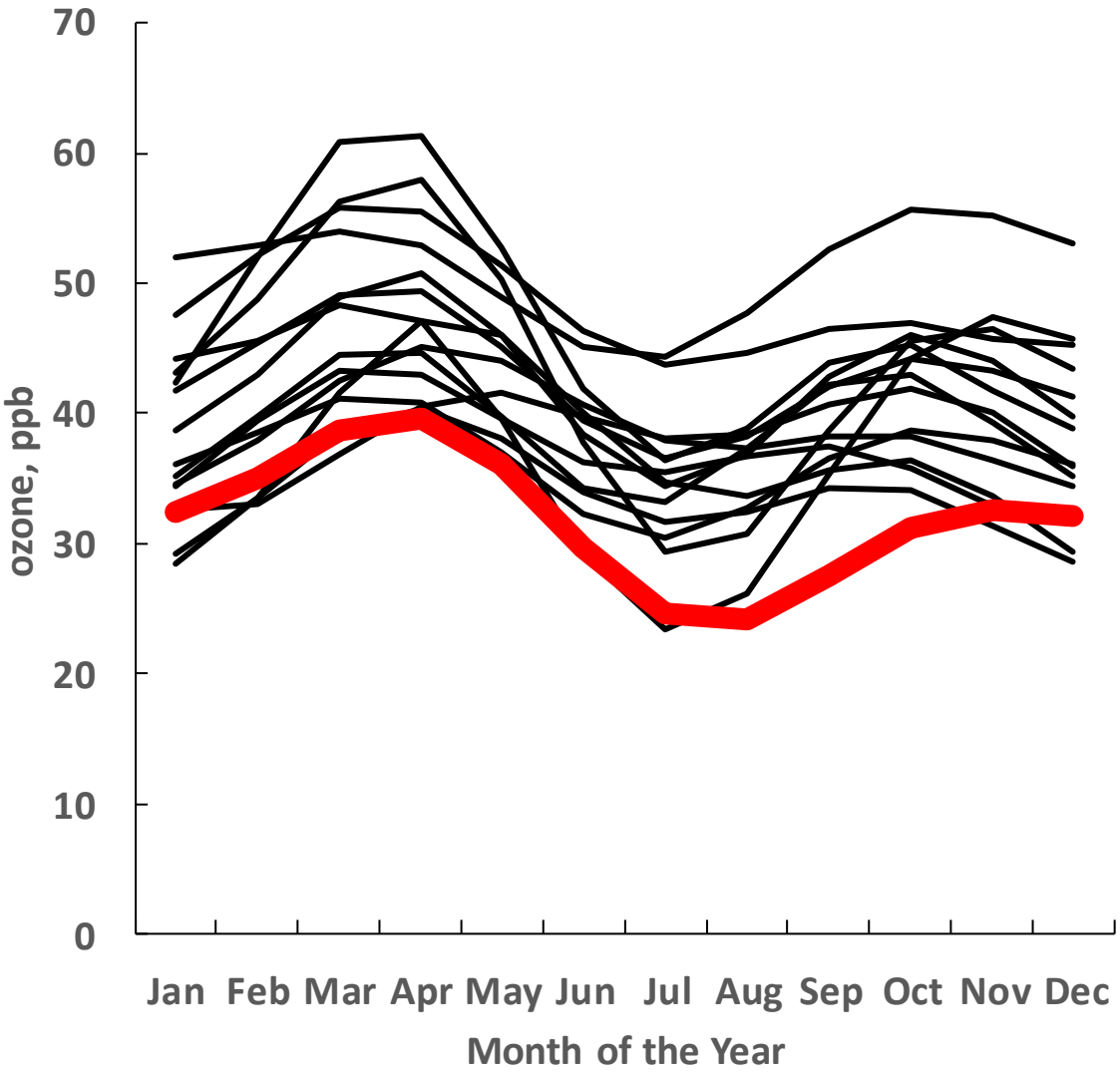

Figure 3b. Seasonal cycles in ozone at the Trinidad Head, California marine boundary layer station in the ACCMIP models (black lines) and in the observations (thick red line).

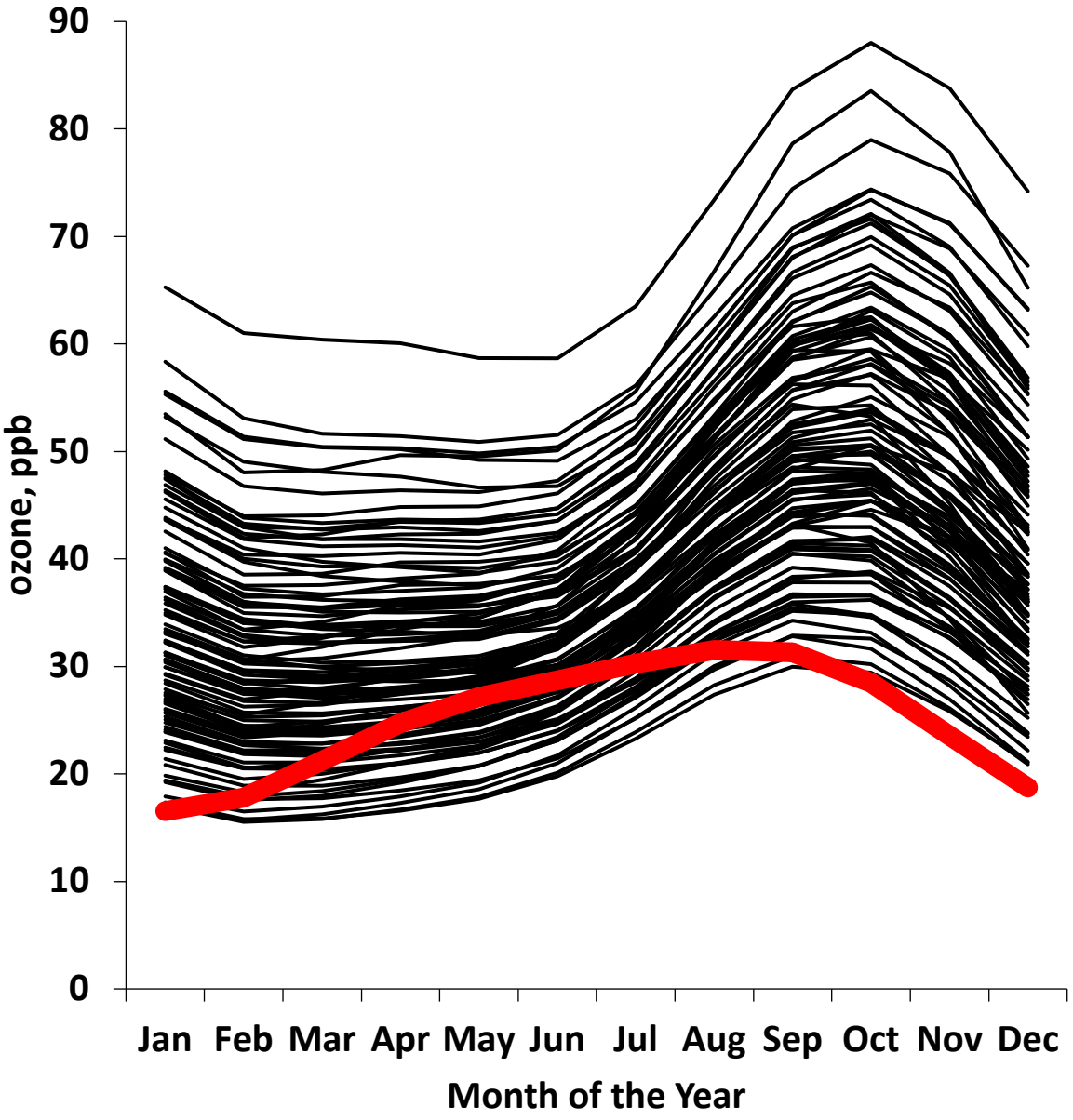

Figure 4a. Seasonal cycles in ozone at the Cape Grim, Tasmania marine boundary layer station in the STOCHEM-OC Monte Carlo model runs (black lines) and in the observations (thick red line).

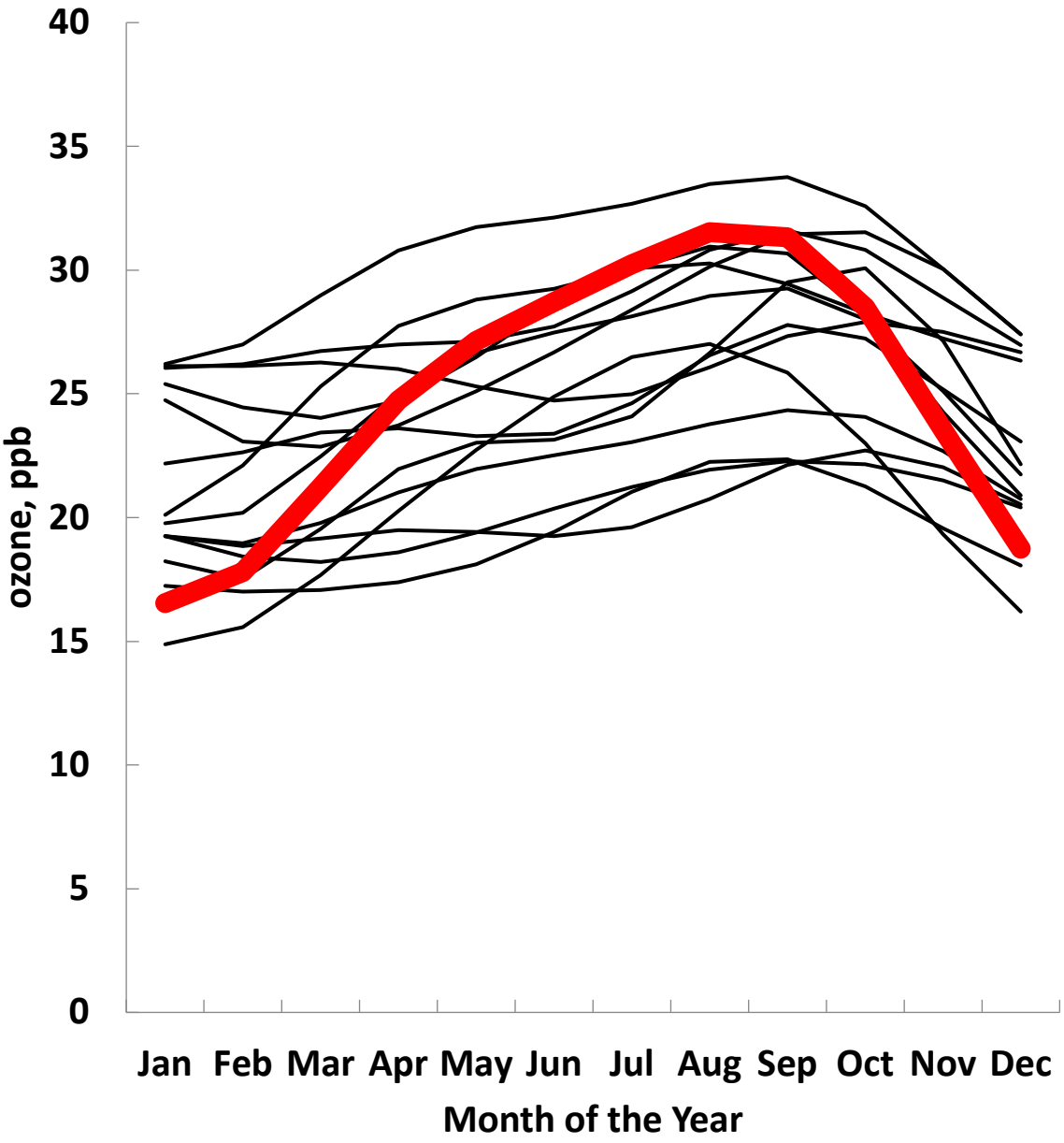

Figure 4b. Seasonal cycles in ozone at the Cape Grim, Tasmania marine boundary layer station in the ACCMIP models (black lines) and in the observations (thick red line).